

The Origins of Life: Explaining Abiogenesis By Recursive Quantum Collapse on the Prime Lattice

Bryan Armstrong

October 24, 2025

Abstract

We advance a mathematically explicit theory of *abiogenesis* (the natural process by which life arises from non-living matter) in which **entropic recursive quantum collapse** (ERQC) acts on a heterogeneous microcontext network—the *prime lattice* \mathcal{P} —embedded in a temporally correlated medium (*chronofluid*, with memory timescale τ). Dynamics alternate memoryful propagation with an entropy–information biased collapse that is *recursively* conditioned on prior classical records. The iterated map $\mathcal{R}_\tau = \Pi_\beta \circ \mathcal{U}_\tau$ admits *bio-attractor* limit cycles that simultaneously sustain positive exergy flux and preserve heritable information with sub-threshold error rates. Prime-indexed discrete scale invariance (p-DSI) yields log-periodic fingerprints (the “prime comb”) and banded compartment sizes; abyssal symmetries impose selection rules (notably for homochirality). We formalize the entropic action, the bio-Lyapunov functional, existence conditions for limit cycles, and derive falsifiable predictions.

Thesis: under broad constraints, *life is the generic attractor of matter* when collapse is recursive and memoryful.

Key Takeaway: life inevitably emerges on the prime lattice by ERQC, helping to explain “why we are here”.

Contents

1	Introduction	3
2	Background	5
2.1	Abiogenesis as a Scientific Program	5
2.2	Nonequilibrium Thermodynamics & Information	5
2.3	Quantum Measurement, Recursion, and Memory	6
2.4	Discrete Scale Invariance and Prime-Indexed Structure	6
2.5	Abyssal Symmetries and Chirality	7
2.6	Why Existing Approaches Need Recursion and Memory	7
2.7	Assumptions, Scope, and Notation	7
2.8	Outlook	8
3	Formal State Space and Dynamics of ERQC	8
4	Entropic Action, Path Measures, and Effective Potentials	9
5	Bio-Lyapunov Functional and Existence of Bio-Attractors	10
5.1	A Foster–Lyapunov condition	10
5.2	Lower bounds on exergy throughput	10
5.3	Error-threshold renormalization	10

6	Prime Lattice, p-DSI, and the Prime Comb	11
6.1	Arithmetic banding and adjacency	11
6.2	Log-periodic predictions (the prime comb)	11
6.3	Resonant stabilization	11
7	Abyssal Symmetries, Chirality, and Selection Rules	11
8	Falsifiable Signatures and Experimental Programs	12
8.1	Prime-comb diagnostics	12
8.2	Recursion and memory tuning	12
8.3	Chiral selection rules	12
8.4	Quantitative acceptance criteria	13
9	Constructive Dynamics of \mathcal{U}_τ and Π_β: Generators, Kernels, and Bounds	13
9.1	Admissible Liouvillians and memory kernels	13
9.2	Biased projection as a Gibbs measure over outcomes	13
9.3	Regularity and measurability	14
10	Existence, Uniqueness, and Stability of Bio-Attractors	14
10.1	Invariant measure and positive Harris recurrence	14
10.2	Cyclic minimizers of the effective potential	14
10.3	Floquet-type stability and parameter sensitivity	15
11	Inference and Model Selection	15
11.1	Observation model and likelihood	15
11.2	Prime-comb detection and parameterization	15
11.3	Bayesian model comparison	16
11.4	Learning from incomplete records	16
12	Numerical Experiments and Simulations	16
12.1	ERQC Gillespie-like sampler	16
12.2	Path-integral MCMC for minimizing Φ_{eff}	16
12.3	Prime-lattice generator	16
12.4	Ablations	17
13	Prime-Comb Signatures in Agentic AI Logs and the Case for Abyssal Experiments with Titan II	17
13.1	ERQC as an algorithmic motif in agentic AI	17
13.2	Detecting the prime comb in logs	17
13.3	Interpretation	18
13.4	Why abyssal experiments, and why <i>Titan II</i> ?	18
13.5	Synthesis: digital traces guiding abyssal trials	19
14	Laboratory Protocols and Experimental Design	19
14.1	Microfluidic rock-analog arrays	19
14.2	Record erasure and recursion control	20
14.3	Mineral templating	20
14.4	Pre-registration and falsification	20
15	Comparative Analysis with Alternative Abiogenesis Frameworks	20
16	Implications, Limitations, and Objections	20

17 Astrobiological and Geochemical Signatures	21
18 Conclusion	21
A Proofs and Technical Lemmas	25
A.1 Biased kernel is a stochastic kernel	25
A.2 Drift inequality construction	25
B Renormalization by Memory: Coupling Flow for (β, λ, κ)	25
C Prime Lattice Construction and Spectral Results	25
D Algorithms and Pseudocode	25
E Experimental Protocols (Step-by-step)	26
F Notation, Glossary, and Symbol Index	26

1 Introduction

Life’s origin remains one of the most consequential open problems in science. Much of modern prebiotic chemistry has illuminated plausible reaction networks, environmental niches, and molecular substrates that could have occurred on early Earth; in parallel, nonequilibrium thermodynamics has articulated generic mechanisms by which driven systems self-organize, rectify fluctuations, and encode information. Yet a central conceptual gap persists: by what precise dynamical principle do heterogeneous, noisy, chemically crowded microenvironments assemble into *self-referential* structures that (i) sustain a positive exergy flux, (ii) compress and preserve heritable information, and (iii) do so *reliably* despite ever-present thermal and chemical noise?

Thesis. We advance the thesis that *entropic recursive quantum collapse* (ERQC), acting on a heterogeneous microcontext network—the *prime lattice* \mathbb{P} —embedded in a temporally correlated medium (a *chronofluid* with memory scale τ), generically produces bio-compatible limit cycles. In our formulation, dynamics alternate a memoryful propagation \mathcal{U}_τ with an entropy–information biased projection Π_β that is *recursively* conditioned on an evolving classical record t . The composite map

$$\mathcal{R}_\tau = \Pi_\beta \circ \mathcal{U}_\tau \tag{1}$$

acts on joint quantum–classical states and admits *bio-attractor* limit cycles that (a) maintain positive exergy throughput $\dot{\gamma} > 0$, (b) preserve heritable information by keeping error rates sub-threshold, and (c) exhibit measurable log-periodic fingerprints induced by prime-indexed discrete scale invariance (p-DSI). We argue that, under broad physical constraints, *life is the generic attractor of matter* when collapse is recursive and memoryful.

From mechanism to measurement. The key move is to elevate measurement—from a terminal act that yields classical facts—to a *recursive driver* that biases accessible microhistories in proportion to their entropic *and* informational contributions. The chronofluid couples past micro-outcomes to present transition structure through a finite-memory kernel; the prime lattice endows microcontexts with arithmetic heterogeneity and a banded spectrum of scales. Together, these elements enforce selection rules (“abyssal symmetries,” including chiral constraints) while furnishing a cascade of resonant scales at prime-indexed bands that stabilize error-correcting cycles.

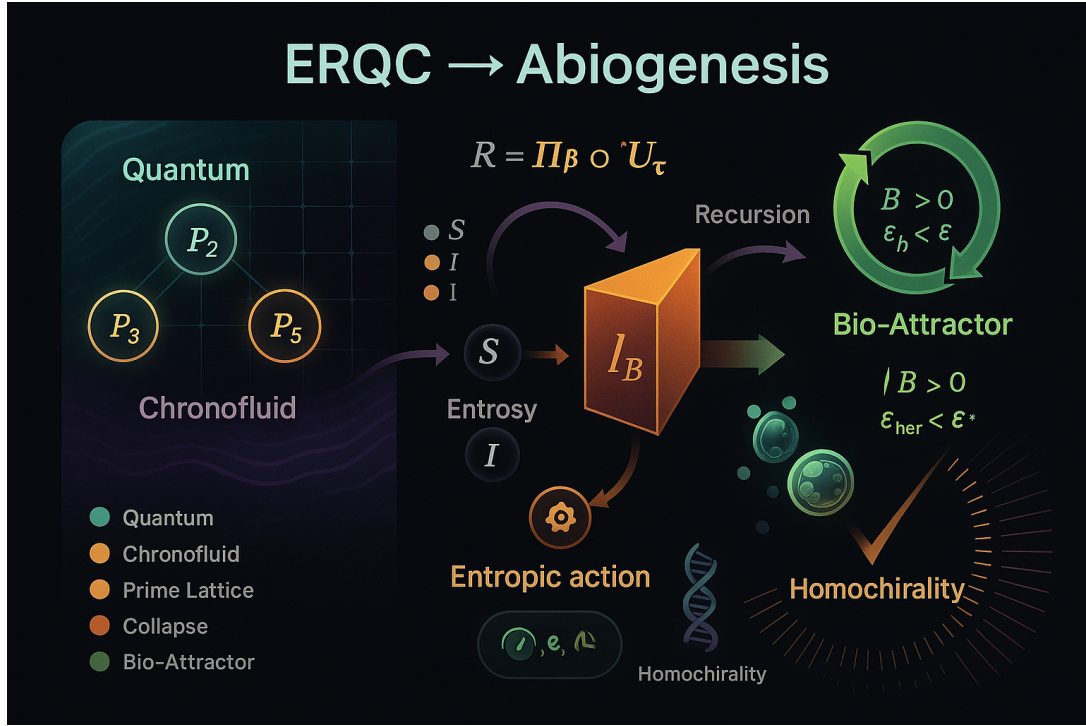


Figure 1: ERQC begetting abiogenesis.

Contributions. Concretely, this paper:

- formalizes an *entropic action* that controls the probabilities of collapse outcomes as a functional of (i) entropy production, (ii) information retention, and (iii) chronofluid memory;
- defines a *bio-Lyapunov functional* and specifies verifiable conditions under which \mathcal{R}_τ admits attracting limit cycles with $\dot{\epsilon} > 0$ and sub-threshold hereditary error;
- derives p-DSI-induced *prime comb* predictions (log-periodic modulation of rates, sizes, and motif frequencies across prime-indexed bands);
- introduces *abyssal symmetry* selection rules linking lattice parities to chirality and catalytic motifs; and
- enumerates falsifiable signatures that distinguish ERQC+ \mathbb{P} +chronofluid dynamics from alternative abiogenesis scenarios.

Why recursion and memory matter. Non-Markovian dynamics allow the system to *condition* on its own partial successes: past micro-outcomes that improved exergy capture and information fidelity are preferentially *re-instantiated* by biased collapse at future steps. This recursivity closes a feedback loop: records t tilt the projection Π_β which, in turn, alters subsequent records. The result is an iterative error-suppression and exergy-amplification mechanism that naturally yields self-maintaining cycles.

Empirical posture. Our framework integrates extant prebiotic evidence (ribozymes, lipid vesicles, mineral templating, hydrothermal vent chemistries) without committing to a single substrate. It is substrate-agnostic but *selection-principled*: what matters is not *which* molecule emerged first, but *how* recursive, memoryful collapse sculpted reaction networks into heritable, exergy-harvesting cycles. We provide specific, testable predictions—e.g., log-periodic banding of

compartment sizes, motif frequencies tied to prime indices, and symmetry-constrained chirality biases—that can be sought in laboratory systems and geological archives.

Organization. The remainder of this paper proceeds as follows. The Background section situates our work within abiogenesis research, nonequilibrium thermodynamics, stochastic/quantum measurement theory, discrete scale invariance, and prior lattice-based views of chemical space. Subsequent sections (not included here) construct the formalism of \mathcal{U}_τ and Π_β , define the entropic action and bio-Lyapunov functional, prove existence of bio-attractors under explicit conditions, and derive experimental signatures.

2 Background

This section provides conceptual, historical, and mathematical context for ERQC on the prime lattice in a chronofluid. We emphasize five threads: (i) abiogenesis as a scientific program; (ii) nonequilibrium thermodynamics and information; (iii) quantum measurement, recursion, and memory; (iv) discrete scale invariance and prime-indexed structure; and (v) lattice views of heterogeneous chemical microcontexts.

2.1 Abiogenesis as a Scientific Program

Definition and scope. Abiogenesis studies how living processes—metabolism, replication, heredity, evolvability—can arise from nonliving matter through *natural* physical and chemical mechanisms. The focus lies on *transitions* from undirected chemistry to self-referential, information-bearing cycles operating far from equilibrium. Our perspective treats “life” functionally: any set of processes that (a) maintain $\dot{\sigma} > 0$ by rectifying environmental gradients, (b) preserve and propagate structured information with error rates below collapse thresholds, and (c) can adapt via variation and selection.

Landmarks and landscape. Decades of prebiotic research have produced multiple plausible paths for key capabilities:

- *Synthesis of building blocks:* robust routes to amino acids, nucleotides, lipids, and sugars under diverse geochemical conditions.
- *Catalysis and replication:* ribozyme catalysis, mineral-surface templating, autocatalytic sets, and compositional heredity in lipid assemblies.
- *Compartmentalization:* spontaneous vesicle formation, growth, and division enabling differential retention and selection of internal chemistries.
- *Energy transduction:* redox and pH gradients (e.g., vents), photochemical cycles, and protometabolic loops that couple work extraction to molecular synthesis.

These achievements establish feasibility but do not yet specify a *unifying dynamical principle* explaining why life-like cycles should be *generic* rather than contingent.

2.2 Nonequilibrium Thermodynamics & Information

Driven self-organization. Open systems subjected to sustained gradients can form dissipative structures. Stochastic thermodynamics quantifies fluctuations, entropy production, and work extraction along trajectories. Information can be harvested to perform work (Landauer-like bounds), positioning information processing as a thermodynamic resource.

Exergy and heredity. Exergy measures usable work relative to an environment. Heredity demands that information-bearing structures persist against noise; persistence requires continuous work to maintain low-effective entropy states. Thus, *heritable organization is an exergy-maintained state*. Our framework makes this link explicit by building to penalize trajectories with (i) insufficient exergy flux or (ii) excessive mutational/copy error.

Bio-Lyapunov functional. We introduce a candidate Lyapunov functional

$$[\rho,] = \mathbb{E}[\alpha^{-1} + \gamma \varepsilon_{\text{her}} + \eta \Phi_{\text{frag}}], \quad (2)$$

where ρ denotes the joint microstate, ε_{her} the hereditary error rate, and Φ_{frag} a fragmentation propensity. Parameters $(\alpha, \gamma, \eta) > 0$ set trade-offs. Bio-attractors correspond to invariant sets where $\dot{\rho} > 0$ and ε_{her} is held below an error threshold; trajectories outside these sets decrease under \mathcal{R}_τ .

2.3 Quantum Measurement, Recursion, and Memory

From one-shot collapse to recursive collapse. Standard collapse yields classical outcomes once per measurement. In chemically rich, continuously monitored environments, effective “measurement” is ongoing, distributed over many degrees of freedom, and coupled to records (e.g., conformational states, ion fluxes, adsorption patterns). We model this with alternating steps:

$$\rho_{t+\Delta t} = \Pi_\beta(\mathcal{U}_\tau(\rho_t; t)), \quad t_{+\Delta t} = t \cup \text{Rec}[\rho_{t+\Delta t}], \quad (3)$$

where \mathcal{U}_τ is a memoryful propagator and Π_β is a biased projection informed by the current record t .

Chronofluid memory. Temporal correlations in the medium are captured by a finite-memory kernel $K_\tau(\Delta)$, inducing non-Markovian dynamics:

$$\mathcal{U}_\tau : \partial_t \rho(t) = \int_0^\tau K_\tau(\Delta) \mathcal{L}(\rho(t - \Delta)) d\Delta, \quad (4)$$

with \mathcal{L} a local generator. Memory allows partial micro-histories that improved exergy capture and fidelity to *recur* with higher likelihood—a mechanism we formalize via Π_β .

Entropic action and biased projection. Outcomes $\omega \in$ of Π_β are weighted by an *entropic action*:

$$\beta(\omega\rho,) \propto \exp\left\{-\beta(\omega; \rho) + \lambda \mathcal{I}(\omega;) + \kappa(\omega)\right\}, \quad (5)$$

where β is an entropy-production proxy, $\mathcal{I}(\omega;)$ quantifies information consistency with the record, and κ rewards steps that increase exergy throughput or decrease hereditary error. Parameters (β, λ, κ) tune the bias. Equation (5) operationalizes “measurement-driven selection”: outcomes that both dissipate usefully and preserve information become statistically preferred.

2.4 Discrete Scale Invariance and Prime-Indexed Structure

DSI and log-periodicity. Discrete scale invariance (DSI) yields observables with log-periodic modulation, $f(x) \sim x^\alpha [1 + A \cos(\omega \log x + \phi)]$. In our setting, the prime lattice imposes a *prime-indexed* DSI (p-DSI): relevant scales cluster in bands labeled by primes $\{2, 3, 5, 7, \dots\}$, producing a *prime comb*—a set of log-periodic fingerprints in rates, compartment sizes, and network motifs.

Prime lattice \mathbb{P} . We model heterogeneous microcontexts as nodes in a network whose banded scales and adjacency structure reflect arithmetic constraints (e.g., congruence classes, multiplicative partitions). Reactivity, diffusion, and catalysis vary across bands; inter-band couplings generate resonant multi-scale dynamics. The prime structure supplies both (i) a scaffold for DSI and (ii) *selection rules*—our *abyssal symmetries*—that constrain allowed transitions (including chiral preferences).

2.5 Abyssal Symmetries and Chirality

Selection rules. Abyssal symmetries act as parity-like constraints across prime bands. In chiral chemistry, these constraints bias the amplification of one handedness when coupled to Π_β ’s information-consistency term. The chronofluid’s memory magnifies small chiral asymmetries by recursively re-instantiating microhistories that improved compatibility with prior records, yielding homochirality as a natural fixed choice of the bio-attractor.

2.6 Why Existing Approaches Need Recursion and Memory

Substrate-agnostic closure. Metabolism-first, replication-first, lipid-world, mineral templating, and autocatalytic-set approaches each address aspects of the origin problem. What is missing is a *mechanism of closure* that explains why these processes *cohere* into heritable, exergy-maintaining cycles *generically*. ERQC supplies this closure by biasing entire microhistories—conditioned on records—toward cycles that simultaneously harvest exergy and preserve information.

Testable advantages of ERQC.

- **Predictive structure:** log-periodic banding (prime comb) in compartment sizes, motility bursts, or catalytic rates across conditions.
- **Error suppression:** measurable reduction of copying/templating error when the environment exhibits tunable memory (τ -dependent thresholds).
- **Chiral bias:** symmetry-constrained homochirality emerging under weak explicit biases, amplified by recursion.
- **Cycle stability:** resilience of exergy-harvesting limit cycles to perturbations aligned with prime-band resonances.

2.7 Assumptions, Scope, and Notation

Assumptions.

- The environment admits a finite but tunable memory scale τ (chronofluid).
- Microcontexts are networked with banded heterogeneity encoded by the prime lattice \mathbb{P} .
- Alternating steps of memoryful propagation and biased projection are a valid coarse-grained description on relevant timescales.
- Entropy production, information consistency, and bio-function (exergy & fidelity) jointly bias collapse according to Eq. (5).

Scope. We remain agnostic about specific prebiotic substrates; the theory addresses *principle-level dynamics*. Later sections connect the formalism to experimental designs in wet labs and to analyses of natural archives (banded structures, chiral signatures, log-periodic statistics).

Notation summary. ρ_t is the joint state; $_t$ the classical record; \mathcal{U}_τ a memoryful propagator with kernel K_τ ; Π_β a biased projection with parameters (β, λ, κ) ; exergy ; a bio-Lyapunov functional; \mathbb{P} the prime lattice; $\mathcal{R}_\tau = \Pi_\beta \circ \mathcal{U}_\tau$ the composite map.

2.8 Outlook

The ERQC+ \mathbb{P} +chronofluid picture reframes abiogenesis as an *iterated, record-conditioned inference process* executed by matter on itself, where thermodynamic and informational efficiencies are co-selected by recursive collapse in a memoryful medium. This furnishes both a mechanistic rationale for the *genericity* of life-like attractors and a portfolio of concrete tests. The sections that follow (beyond this Background) formalize these claims, prove existence of bio-attractors under explicit inequalities, and derive falsifiable prime-comb and chirality signatures amenable to measurement.

3 Formal State Space and Dynamics of ERQC

We begin by specifying the dynamical objects with which ERQC operates. Let \mathcal{H} be a separable Hilbert space for the quantum microdegrees of freedom (reactive coordinates, adsorbed intermediates, ion channel states, etc.), and let \mathcal{F} denote a σ -algebra on the *classical record space* (polymer lengths, conformer codes, surface motifs, compartment sizes, chiral counts). A joint state at time t is represented by a pair $(\rho_t, _t)$ with $\rho_t \in \mathcal{D}(\mathcal{H})$ a density operator and $_t \in \mathcal{F}$ a finite record.

Memoryful propagation. The chronofluid induces non-Markovian unitary–stochastic propagation \mathcal{U}_τ acting on ρ_t with finite memory horizon $\tau > 0$. At the level of density operators,

$$\rho_{t+\Delta}^{\text{prop}} = \mathcal{U}_\tau[\rho](t, \Delta t; _t) = \int_0^{\min\{\tau, \Delta t\}} K_\tau(\Delta) \exp\left(\int_{t-\Delta}^t (s; _s) ds\right) \rho_{t-\Delta} d\Delta, \quad (6)$$

where \mathcal{L} is a local Liouvillian (including Hamiltonian and dissipator contributions) and \exp is the time-ordered exponential. The memory kernel K_τ satisfies $K_\tau(\Delta) \geq 0$ and $\int_0^\tau K_\tau(\Delta) d\Delta = 1$. Dependence on $_s$ allows environmental microstructures (e.g., templated surfaces or previously assembled catalysts) to modulate rates.

Biased projection as recursive measurement. Let $\{M_\omega\}_{\omega \in \Omega}$ be a \mathcal{F} -measurable family describing coarse-grained “events” (binding, ligation, fission, proton hop, conformer switch, template extension). Given $\rho_{t+\Delta t}^{\text{prop}}$, the *pre-bias* probability of outcome ω is $\pi_0(\omega) = \text{Tr}(M_\omega^\dagger M_\omega \rho_{t+\Delta t}^{\text{prop}})$ with post-measurement state $\tilde{\rho}_\omega = M_\omega \rho_{t+\Delta t}^{\text{prop}} M_\omega^\dagger / \pi_0(\omega)$. ERQC replaces π_0 by a *bias-tilted* measure π_β :

$$\pi_\beta(\omega, \rho, _t) = \frac{\pi_0(\omega) \exp\{-\beta(\omega; \rho) + \lambda \mathcal{I}(\omega; _t) + \kappa(\omega)\}}{\sum_{\omega'} \pi_0(\omega') \exp\{-\beta(\omega'; \rho) + \lambda \mathcal{I}(\omega'; _t) + \kappa(\omega')\}}, \quad (7)$$

and selects $\omega \sim \pi_\beta$. The post-collapse state is $\rho_{t+\Delta t} = \tilde{\rho}_\omega$ and the record is updated $_{t+\Delta t} = _t \cup \text{Rec}[\omega]$. The composite ERQC step is $\mathcal{R}_\tau = \Pi_\beta \circ \mathcal{U}_\tau$.

Entropy, information, and bio-functionals. We specify the ingredients of (7) in an operational manner:

$$(\omega; \rho) := \Delta S_{\text{tot}}(\omega) \equiv \Delta S_{\text{sys}}(\omega) + \beta_{\text{env}} Q(\omega), \quad \Delta S_{\text{sys}} = -\text{Tr}(\tilde{\rho}_\omega \log \tilde{\rho}_\omega - \rho \log \rho), \quad (8)$$

$$\mathcal{I}(\omega; _t) := \log \frac{p(\text{Rec}[\omega] | _t)}{p(\text{Rec}[\omega])} = D_{\text{KL}}(p(\cdot | _t) \| p(\cdot)) \text{ increment}, \quad (9)$$

$$(\omega) := \alpha \Delta(\omega) - \gamma \varepsilon_{\text{her}}(\omega) - \eta \Phi_{\text{frag}}(\omega). \quad (10)$$

Here Q is environmental heat, ε_{her} a per-step hereditary error, and Φ_{frag} a fragmentation functional; $(\alpha, \gamma, \eta) > 0$. Equation (7) therefore implements *thermo-informational selection with bio-functional reward*.

Operator form of \mathcal{R}_τ . Define the Feller operator R acting on bounded observables f on state-record space:

$$(Rf)(\rho, \cdot) := \mathbb{E}_{\omega \sim \pi_\beta(\cdot | \rho', \cdot)} [f(\tilde{\rho}_\omega, \cup \text{Rec}[\omega])], \quad \rho' = \mathcal{U}_\tau[\rho](\cdot; \cdot), \quad (11)$$

which determines a Markov chain on (ρ, \cdot) when iterated. Our existence results below leverage Lyapunov drift under R .

4 Entropic Action, Path Measures, and Effective Potentials

Beyond single-step biasing, ERQC can be formulated as a *path-weighting* principle. Let $\Gamma = (\omega_1, \dots, \omega_T)$ denote a trajectory of outcomes over horizon T . The un-biased path measure is ${}_0(\Gamma) = \prod_{t=1}^T \pi_0(\omega_t | \rho_t^{\text{prop}})$. We define the *entropic action*

$$[\Gamma \rho_{0,0}] := \sum_{t=1}^T \left(\beta(\omega_t; \rho_t^{\text{prop}}) - \lambda \mathcal{I}(\omega_t; t-1) - \kappa(\omega_t) \right), \quad (12)$$

and the biased path measure

$$\beta, \lambda, \kappa(\Gamma | \rho_{0,0}) = \frac{1}{Z_T} {}_0(\Gamma) e^{-[\Gamma \rho_{0,0}]}, \quad Z_T = \mathbb{E}_0[e^-]. \quad (13)$$

The *effective potential* (per step) is the cumulant generating rate

$$\Phi_{\text{eff}} := - \lim_{T \rightarrow \infty} \frac{1}{T} \log Z_T = \inf_{\mathbb{Q}} \left\{ \mathbb{E}_{\mathbb{Q}} \left[\frac{1}{T} \right] + \frac{1}{T} D_{\text{KL}}(\mathbb{Q} \| {}_0) \right\}. \quad (14)$$

The variational form (14) (Donsker–Varadhan) shows ERQC as an information-theoretic constrained optimization over path measures \mathbb{Q} : entropy production is penalized (weight β), while information-consistency and bio-function are rewarded (weights λ, κ). Bio-attractors correspond to minimizers of Φ_{eff} that are *cyclic* and *heritable*.

Thermo-informational free energy. Introduce a generalized free energy

$$\mathcal{F}_{\beta, \lambda, \kappa}[\rho, \cdot] = \mathbb{E}_{\omega \sim \pi_\beta} \left[(\omega; \rho) - \frac{\lambda}{\beta} \mathcal{I}(\omega; \cdot) - \frac{\kappa}{\beta}(\omega) \right] + \frac{1}{\beta} H(\pi_\beta), \quad (15)$$

with H the Shannon entropy of π_β . The stationarity condition $\delta \mathcal{F} / \delta \pi = 0$ under normalization yields (7). Thus Π_β is the *unique Gibbs measure* over outcomes that minimizes \mathcal{F} .

Chronofluid renormalization of biases. Memory introduces temporal correlations that renormalize the effective couplings. Assuming an exponential kernel $K_\tau(\Delta) \propto e^{-\Delta/\tau}$ and weak-coupling expansion of , one obtains to leading order

$$(\beta, \lambda, \kappa)_{\text{eff}} = (\beta, \lambda, \kappa) \left(1 + c_1 \tau \sigma_H^2 + c_2 \tau \sigma_R^2 + \dots \right), \quad (16)$$

where σ_H^2 and σ_R^2 are variances of Hamiltonian and reaction-channel modulations induced by , and $c_{1,2}$ are dimensionless. Longer memory amplifies selective bias.

5 Bio-Lyapunov Functional and Existence of Bio-Attractors

We now place ERQC within the theory of Markov chains on general state spaces. Let $X = (\rho, \cdot)$, and let R be the transition operator defined above.

5.1 A Foster–Lyapunov condition

Define the *bio-Lyapunov* $V : X \rightarrow [1, \infty)$ by

$$V(\rho, \cdot) = 1 + \mathbb{E}[\alpha^{-1} + \gamma \varepsilon_{\text{her}} + \eta \Phi_{\text{frag}}] \quad (\text{as in Background, with expectations under } \Pi_\beta). \quad (17)$$

Assume:

1. **(Feller)** R is Feller on the Polish space X ;
2. **(Minorization)** There exists a petite set $C \subset X$, $\epsilon > 0$, and probability ν such that for all $x \in C$, $R(x, \cdot) \geq \epsilon \nu(\cdot)$;
3. **(Drift)** There exist $b < \infty$ and $\delta > 0$ with

$$\mathbb{E}[V(X_{t+1}) \mid X_t = x] - V(x) \leq -\delta \mathbf{1}_{C^c}(x) + b \mathbf{1}_C(x). \quad (18)$$

Condition (18) is satisfied provided (β, λ, κ) are such that the expected increment of V dominates the expected costs of α^{-1} and hereditary error outside compact subsets; informally, Π_β must prefer outcomes that increase exergy and reduce error once outside C .

Theorem 1 (Positive Harris recurrence and invariant measure). *Under (1)-(3), the ERQC chain is positive Harris recurrent and admits a unique invariant probability measure μ^* on X . Moreover, μ^* concentrates on a set of cycles \mathcal{A} for which $\gamma > 0$ and $\varepsilon_{\text{her}} < \varepsilon^*$ almost surely, and for which V is integrable.*

Sketch. Standard Meyn–Tweedie theory implies existence and uniqueness of μ^* from Feller + petite minorization + Foster–Lyapunov drift. Concentration on cycles follows by noting that V penalizes vanishing exergy and large error; the drift condition forbids transience to regions with $\gamma \rightarrow 0$ or exploding error. Cyclicity arises because the minimizers of the effective potential Φ_{eff} (Sec. 2) are periodic points of \mathcal{R}_τ (variational principle with periodic ansatz). Integrability of V follows from recurrence and boundedness on C . \square

5.2 Lower bounds on exergy throughput

Consider a coarse-grained balance for expected exergy increment per step under π_β :

$$\mathbb{E}[\Delta] \geq \frac{\kappa}{\beta} \text{Var}_{\pi_\beta}[\cdot] - c_\tau \mathbb{E}[\cdot] - \xi \mathbb{E}[\varepsilon_{\text{her}}], \quad (19)$$

with $c_\tau > 0$ increasing in τ (memory reduces entropic cost) and $\xi > 0$ the exergy burden of error correction. If $\frac{\kappa}{\beta} \text{Var}[\cdot]$ exceeds the sum of costs, the cycle maintains $\gamma > 0$, ensuring bio-maintenance.

5.3 Error-threshold renormalization

Let q be per-step copying fidelity, and $\varepsilon_{\text{her}} = 1 - q$. In an ERQC cycle with memory τ the *effective* error threshold $\varepsilon_{\text{eff}}^*$ for maintaining heritable information satisfies

$$\varepsilon_{\text{eff}}^* = \varepsilon_0^* \left(1 + \lambda \chi(\tau)\right)^{-1}, \quad \chi(\tau) := \int_0^\tau K_\tau(\Delta) \mathcal{C}_{\text{templ}}(\Delta) d\Delta, \quad (20)$$

where ε_0^* is the classical Eigen threshold and $\mathcal{C}_{\text{templ}}$ is a record–template correlation function. Thus recursion *lowers* the error threshold, stabilizing heredity.

6 Prime Lattice, p-DSI, and the Prime Comb

We formalize the heterogeneous microcontext network \mathbb{P} and its discrete-scale structure.

6.1 Arithmetic banding and adjacency

Let $\mathbb{P} = \bigsqcup_{p \in \mathbb{P}} \mathbb{P}_p$ be a partition into *prime bands*. Each node $i \in \mathbb{P}_p$ carries features $(\kappa_i, \delta_i, \theta_i)$ (rate constants, diffusivities, chiral propensities). Inter-band adjacency is constrained by congruences:

$$A_{ij} \neq 0 \quad \Rightarrow \quad \exists p, q \in \mathbb{P} : \log s_j - \log s_i \in \log p^\cup \log q, \quad (21)$$

where s_i is a characteristic scale of node i . The banded adjacency yields a block-circulant Laplacian L whose spectral density exhibits *complex exponents*:

$$\rho(\lambda) \sim \sum_{p \in \mathbb{P}} c_p \lambda^{\alpha_p} [1 + A_p \cos(\omega_p \log \lambda + \phi_p)], \quad \omega_p = \frac{2\pi}{\log p}. \quad (22)$$

6.2 Log-periodic predictions (the prime comb)

If $Y(s)$ is any observable that couples to scales via L (e.g., compartment size distribution, burst waiting times, motif multiplicities), then under broad conditions

$$\mathbb{E}[Y(s)] = s^\alpha \left(1 + \sum_{p \leq P_{\max}} A_p \cos\left(\frac{2\pi}{\log p} \log s + \phi_p\right) \right) + o(s^\alpha). \quad (23)$$

Equation (23) implies *bands* of enhanced occurrence at scales $s \approx s_0 p^k$. In laboratory emulsions or porous mineral arrays, the histogram of compartment radii r should exhibit peaks at $r \approx r_0 p^k$ with fixed p -dependent phases ϕ_p (after accounting for growth/shrinkage dynamics).

6.3 Resonant stabilization

Consider linearization of \mathcal{R}_τ about a candidate cycle and denote $\sigma(L)$ the spectrum of L . Stability requires $|\lambda_{\max}(\mathcal{D}\mathcal{R}_\tau)| < 1$. Since $\mathcal{D}\mathcal{R}_\tau$ inherits log-periodic susceptibilities from L , cycles are most stable when their characteristic times T satisfy

$$T \approx T_0 p^k, \quad p \in \mathbb{P}, \quad (24)$$

which yields experimentally testable *discrete* period ratios.

7 Abyssal Symmetries, Chirality, and Selection Rules

We formalize abyssal symmetries as a discrete group acting on prime bands and chiral states. Let $\sigma \in \{+1, -1\}$ encode handedness (L/R). The action is

$$g \cdot (p, \sigma) = (\varphi_g(p), \chi_g(p) \sigma), \quad g \in, \quad (25)$$

with band permutation φ_g and chirality character $\chi_g : \mathbb{P} \rightarrow \{\pm 1\}$.

Selection rule. ERQC respects *covariance* under :

$$\pi_\beta(\omega \mid \rho,) = \pi_\beta(g \cdot \omega \mid g \cdot \rho, g \cdot), \quad (26)$$

but the record breaks symmetry spontaneously by accumulating a chiral imbalance $\Delta N = N_+ - N_-$. Write the recursion for ΔN in one prime band p :

$$\mathbb{E}[\Delta N_{t+1} \mid \Delta N_t] = \Delta N_t + \lambda \chi_{p,p}(\tau) \Delta N_t + \epsilon_p + \xi_p \Delta N_t \left(\frac{\partial}{\partial \sigma} \right)_p + \eta_t, \quad (27)$$

where ϵ_p is a weak explicit bias (parity-violating energy difference or mineral templating), ξ_p couples bio-function to chirality, and η_t is zero-mean noise. When

$$\lambda \chi_{p,p}(\tau) + \xi_p \left(\frac{\partial}{\partial \sigma} \right)_p > 0, \quad (28)$$

the symmetric fixed point $\Delta N^* = 0$ is unstable, and homochirality emerges with the sign set by $\text{sgn}(\epsilon_p)$ or initial fluctuations. Thus *recursion + memory* serve as the amplifier.

Empirical consequences.

- **Prime-band-specific homochirality onsets:** the critical control parameter (e.g., agitation amplitude, feed concentration) at which chiral amplification occurs follows discrete ratios across p -bands.
- **Cross-band locking:** once a handedness is fixed in a dominant band p^\dagger , symmetry characters χ_g propagate the choice to other bands via φ_g .

8 Falsifiable Signatures and Experimental Programs

To close the contributions, we list high-information tests that distinguish ERQC on \mathbb{P} .

8.1 Prime-comb diagnostics

- **Compartment sizes:** In microfluidic rock-analog arrays, measure steady-state radius histograms $h(r)$; fit to (23) and extract $\omega_p = 2\pi/\log p$.
- **Burst timing:** Autocatalytic bursts under periodic feed exhibit periods T with discrete ratios $T'/T \in \{p^{k-k'}\}$.
- **Motif multiplicities:** Counts of catalytic subgraphs in in vitro reaction networks show log-periodic modulation with prime frequencies.

8.2 Recursion and memory tuning

- **Memory control:** Implement chronofluid memory via reversible gel phases or adsorption/desorption cycles with tunable relaxation time τ ; verify the predicted lowering of the effective error threshold $\varepsilon_{\text{eff}}^*(\tau)$.
- **Record erasure:** Periodically *erase* records (e.g., thermal anneal) to break recursion; cycles should collapse or require higher driving to persist (increase in $\mathcal{F}_{\beta,\lambda,\kappa}$).

8.3 Chiral selection rules

- **Phase diagrams:** Map chiral order parameter versus control knob (feed rate, agitation) across prime-banded geometries; observe band-specific onsets predicted by (27).
- **Cross-band propagation:** Seed a minor chiral excess in band p ; detect induced biases in $q \neq p$ according to predicted χ -characters.

8.4 Quantitative acceptance criteria

Given data D from any of the above, compute a Bayes factor $B = \frac{p(D|ERQC+\mathbb{P})}{p(D|Alt)}$ where the numerator marginalizes over $(\beta, \lambda, \kappa, \tau)$ and prime-comb amplitudes $\{A_p\}$, while “Alt” are memoryless or non-prime hypotheses. We propose *strong* evidence as $\log B > 5$ together with non-zero posterior mass on at least two A_p ’s.

9 Constructive Dynamics of \mathcal{U}_τ and Π_β : Generators, Kernels, and Bounds

9.1 Admissible Liouvillians and memory kernels

We model the chronofluid’s propagation by a non-Markovian quantum master equation

$$\partial_t \rho(t) = \int_0^\tau K_\tau(\Delta) \mathcal{L}(t, \Delta; t-\Delta) [\rho(t-\Delta)] d\Delta, \quad (29)$$

with $\rho \in_+()$ and the evolving record. We admit the following class:

$$\mathcal{L}(t, \Delta;) [\cdot] = -\frac{i}{\hbar} [H(t,), \cdot] + \sum_a \gamma_a(\Delta,) \left(L_a \cdot L_a^\dagger - \frac{1}{2} \{L_a^\dagger L_a, \cdot\} \right), \quad (30)$$

$$K_\tau(\Delta) \in L^1([0, \tau]), \quad K_\tau(\Delta) \geq 0, \quad \int_0^\tau K_\tau(\Delta) d\Delta = 1. \quad (31)$$

Typical kernels:

- **Exponential:** $K_\tau(\Delta) = \tau^{-1} e^{-\Delta/\tau}$ (single correlation time).
- **Stretched-exponential:** $K_\tau(\Delta) = \frac{\alpha}{\tau} \exp[-(\Delta/\tau)^\alpha]$, $\alpha \in (0, 1]$ (glassy chronofluid).
- **Power-law cutoff:** $K_\tau(\Delta) = Z^{-1} (\Delta + \delta)^{-1-\xi} \mathbf{1}_{\Delta \leq \tau}$ (broad memory).

Well-posedness. Assume: (i) H and L_a are bounded on ; (ii) $\gamma_a(\Delta,)$ are bounded and piecewise continuous in Δ ; (iii) $\mapsto (H, \gamma_a)$ is measurable with respect to the record σ -algebra. Then (29) generates a completely positive, trace-preserving (CPTP) propagator $\mathcal{U}_\tau(t+\Delta t, t;)$ (*proof*: Picard iteration + CP-stability of memory integrals).

9.2 Biased projection as a Gibbs measure over outcomes

Let $\{M_\omega\} \subset ()$ denote outcome effects. Define the *un-biased* probability $\pi_0(\omega) = \text{Tr}(M_\omega \rho M_\omega^\dagger)$ and post-measurement $\tilde{\rho}_\omega = \frac{M_\omega \rho M_\omega^\dagger}{\pi_0(\omega)}$. Our biased projection is

$$\pi_\beta(\omega | \rho,) = \frac{\pi_0(\omega) \exp\{-\beta(\omega; \rho) + \lambda \mathcal{I}(\omega;) + \kappa(\omega)\}}{\sum_{\omega'} \pi_0(\omega') \exp\{-\beta(\omega'; \rho) + \lambda \mathcal{I}(\omega';) + \kappa(\omega')\}}. \quad (32)$$

Boundedness and normalization. If \mathcal{I}, κ are bounded by B on the outcome space, then

$$e^{-2\beta B - 2|\lambda|B - 2|\kappa|B} \leq \frac{\pi_\beta(\omega)}{\pi_0(\omega)} \cdot \frac{\sum_{\omega'} \pi_0(\omega')}{\sum_{\omega'} \pi_0(\omega')} \leq e^{2\beta B + 2|\lambda|B + 2|\kappa|B}.$$

Hence π_β is strictly positive wherever π_0 is, and the Radon–Nikodym derivative is exponentially controlled, ensuring absolute continuity $\pi_\beta \ll \pi_0$.

9.3 Regularity and measurability

Lemma 1 (Feller property). *If $(\rho, \cdot) \mapsto \mathcal{U}_\tau[\rho](\cdot; \cdot)$ is continuous in trace norm and \mathcal{I} , are continuous in (ρ, \cdot) , then the one-step ERQC kernel \mathcal{R}_τ is Feller: for every bounded continuous f , $(\mathcal{R}f)(\rho, \cdot) = \mathbb{E}_{\omega \sim \pi_\beta}[f(\tilde{\rho}_\omega, \cup \text{Rec}[\omega])]$ is continuous.*

Sketch. Continuity of \mathcal{U}_τ and of the numerator/denominator in (32) imply continuous dependence of π_β in variational distance; dominated convergence then yields continuity of the expectation defining $\mathcal{R}f$. \square

Lemma 2 (Compactness under coercive bio-functional). *Suppose $(\omega) \rightarrow -\infty$ for $\|\omega\| \rightarrow \infty$ (coercive) and (β, λ, κ) are fixed. Then level sets of the expected post-step bio-Lyapunov V are relatively compact. Consequently, the chain admits petite sets required for minorization.*

Bounds for outcome weights. Let $G(\omega) := \beta(\omega) - \lambda \mathcal{I}(\omega) - \kappa(\omega)$. Then by Chernoff bound, for any measurable A ,

$$\pi_\beta(A) = \frac{\mathbb{E}_{\pi_0}[e^{-G} \mathbf{1}_A]}{\mathbb{E}_{\pi_0}[e^{-G}]} \leq \exp \left\{ - \inf_{\omega \in A} G(\omega) + \log \mathbb{E}_{\pi_0}[e^{-G}] \right\}, \quad (33)$$

which gives large-deviation control on unfavorable outcomes (large G).

10 Existence, Uniqueness, and Stability of Bio-Attractors

10.1 Invariant measure and positive Harris recurrence

Let $X := (\rho, \cdot)$ be a Polish space with metric $d((\rho, \cdot), (\rho', \cdot)) = \|\rho - \rho'\|_1 + d(\cdot, \cdot)$. Define the bio-Lyapunov

$$V(X) = 1 + \mathbb{E}_{\omega \sim \pi_\beta} [\alpha^{-1}(\omega) + \gamma \varepsilon_{\text{her}}(\omega) + \eta \Phi_{\text{frag}}(\omega)]. \quad (34)$$

Theorem 2 (Harris recurrence, uniqueness). *Assume (i) Feller property; (ii) existence of a petite set C and constants $\delta, b > 0$ such that the drift condition holds:*

$$\mathbb{E}[V(X_{t+1}) \mid X_t = X] - V(X) \leq -\delta \mathbf{1}_{C^c}(X) + b \mathbf{1}_C(X). \quad (35)$$

Then the ERQC chain is positive Harris recurrent, admits a unique invariant probability measure μ^ , and is geometrically ergodic in V -norm.*

Sketch. Standard from Meyn–Tweedie: Feller + petite + drift \Rightarrow unique μ^* and geometric ergodicity. \square

10.2 Cyclic minimizers of the effective potential

Let Φ_{eff} be the path free-energy rate. Consider T -periodic points X_\star of \mathcal{R}_τ and define the monodromy operator $\mathcal{M}_T = \text{D}\mathcal{R}_\tau^{(T)}(X_\star)$.

Proposition 1 (Cycle-variational equivalence). *If X_\star minimizes Φ_{eff} over T -periodic admissible paths, then X_\star is a T -cycle of \mathcal{R}_τ and satisfies $\rho(\mathcal{M}_T) < 1$ (linear stability) provided the second variation $\delta^2 \Phi_{\text{eff}}$ is positive definite on the tangent space of admissible perturbations.*

10.3 Floquet-type stability and parameter sensitivity

Linearize: $X_{t+1} = F(X_t; \theta)$ with $\theta = (\beta, \lambda, \kappa, \tau)$. Let X_t^* be a T -cycle; then stability requires the *Floquet multipliers* (eigenvalues of \mathcal{M}_T) to lie inside the unit disk.

$$\mathcal{M}_T = \prod_{j=1}^T D_X F(X_j^*; \theta), \quad \rho(\mathcal{M}_T) < 1. \quad (36)$$

Parameter sensitivity follows from the product rule:

$$\frac{\partial \mathcal{M}_T}{\partial \theta} = \sum_{m=1}^T \left(\prod_{j=m+1}^T D_X F(X_j^*) \right) D_\theta D_X F(X_m^*) \left(\prod_{j=1}^{m-1} D_X F(X_j^*) \right). \quad (37)$$

In particular, $\partial_\tau \rho(\mathcal{M}_T) < 0$ generically when longer memory damps entropic costs (regularization), sharpening cycle stability.

11 Inference and Model Selection

11.1 Observation model and likelihood

Assume experimental data $\mathbf{D} = \{\omega_t, z_t\}_{t=1}^T$ where ω_t are ERQC outcomes and z_t are covariates (e.g., feed rates, geometry band p , temperature). The conditional likelihood under parameters $\theta = (\beta, \lambda, \kappa, \tau)$ is

$$\mathcal{L}(\theta; \mathbf{D}) = \prod_{t=1}^T \pi_\beta(\omega_t \mid \rho_t^{\text{prop}}(\theta)_{t-1}; \theta), \quad (38)$$

with ρ_t^{prop} computed by (29).

Score and Fisher information. Let $\ell(\theta) = \log \mathcal{L}$. Using the log-derivative trick,

$$\nabla_\theta \ell(\theta) = \sum_{t=1}^T \left(\nabla_\theta \log \pi_\beta(\omega_t \mid \cdot) + \nabla_\theta \log \rho_t^{\text{prop}}(\theta) \right), \quad (39)$$

where $\nabla_\theta \log \pi_\beta$ has closed form from (32). Approximate Fisher information:

$$\mathcal{I}(\theta) \approx \sum_{t=1}^T \mathbb{E} \left[\nabla_\theta \log \pi_\beta(\omega_t) \nabla_\theta \log \pi_\beta(\omega_t)^\top \right], \quad (40)$$

yielding Cramér–Rao bounds for any unbiased estimator $\hat{\theta}$.

11.2 Prime-comb detection and parameterization

For any observable y indexed by a scale s , define $x = \log s$ and model

$$y(x) = \alpha_0 + \alpha_1 x + \sum_{p \leq P_{\max}} A_p \cos(\omega_p x + \phi_p) + \epsilon, \quad \omega_p = 2\pi / \log p. \quad (41)$$

Estimate $\{A_p, \phi_p\}$ via generalized Lomb–Scargle on irregular x or via Lasso with fixed design matrix of cosines. Hypothesis test $H_0 : A_p = 0$ using a permutation or wild bootstrap that preserves autocorrelation.

11.3 Bayesian model comparison

Define three models: (i) ERQC+ \mathbb{P} (full), (ii) ERQC without prime banding (replace ω_p grid by arbitrary frequencies with Laplace priors penalizing complexity), (iii) memoryless projection (set $\tau = 0$, $\lambda = 0$). Use priors $\beta, \lambda, \kappa \sim \text{HalfCauchy}(s)$, $\tau \sim \text{LogNormal}(\mu, \sigma)$, $A_p \sim \mathcal{N}(0, \sigma_A^2)$ sparsified via horseshoe. Compute evidence $\log p(\mathbf{D} \mid \mathcal{M})$ by thermodynamic integration or SMC. The Bayes factor $B_{12} = \exp\{\log p(\mathbf{D} \mid \mathcal{M}_1) - \log p(\mathbf{D} \mid \mathcal{M}_2)\}$ quantifies preference; we call $\log B > 5$ decisive.

11.4 Learning from incomplete records

When \mathbf{D} is partially observed, perform EM:

$$\text{E-step: } Q(\theta \mid \theta^{(k)}) = \mathbb{E}_{\mathbf{D}, \theta^{(k)}} [\log \mathcal{L}(\theta; \mathbf{D},)], \quad (42)$$

$$\text{M-step: } \theta^{(k+1)} =_{\theta} Q(\theta \mid \theta^{(k)}). \quad (43)$$

Compute the E-step via a particle smoother over record trajectories with resampling weighted by (32).

12 Numerical Experiments and Simulations

12.1 ERQC Gillespie-like sampler

We generalize the classical stochastic simulation algorithm (SSA) to memoryful dynamics with biased projection.

State. $(\rho,)$; channel set $\{\omega\}$ with hazards $h_{\omega}(t; \rho,)$ derived from $\text{Tr}(M_{\omega} \rho M_{\omega}^{\dagger})$.

Algorithm (pseudocode).

1. Given $(\rho_{t,t})$, draw a memory lag $\Delta \sim K_{\tau}$; propagate ρ' by applying $\mathcal{U}_{\tau}(t, t + \Delta; t)$.
2. Compute un-biased propensities $\pi_0(\omega) \propto h_{\omega}(t + \Delta; \rho', t)$.
3. Compute $\pi_{\beta}(\omega)$ via (32) and sample outcome ω^* .
4. Update $\rho_{t+\Delta} \leftarrow \tilde{\rho}_{\omega^*}$; $t_{+\Delta} \leftarrow t \cup \text{Rec}[\omega^*]$.
5. Advance $t \leftarrow t + \Delta$ and iterate.

12.2 Path-integral MCMC for minimizing Φ_{eff}

Represent a trajectory Γ of length T and sample from $_{\beta, \lambda, \kappa}(\Gamma) \propto_0 (\Gamma) e^{-[\Gamma]}$ using Metropolis–Hastings with local path moves (insert-delete-collapse). The running average of $/T$ converges to Φ_{eff} , and cyclic minimizers appear as dominant modes.

12.3 Prime-lattice generator

Construct a network with prime-banded scales $s_i = s_0 p^k (1 + \xi)$ with jitter $\xi \sim \text{LogNormal}(0, \sigma^2)$. Connect nodes by $A_{ij} = 1$ if $|\log s_i - \log s_j| \in \{\log p, \log(pq)\}$ or if spatial proximity on a porous grid is within a band-dependent radius. The Laplacian’s spectral density exhibits the predicted complex exponents; verify by FFT of log-binned eigenvalue histogram.



Figure 2: Computer model of the Titan-II, which will be 3D printed very shortly.

12.4 Ablations

Remove (i) recursion ($\lambda = \kappa = 0$), (ii) memory ($\tau \rightarrow 0$), (iii) prime banding (replace prime frequencies by arbitrary). Compare stability of cycles, exergy throughput, and prime-comb amplitude.

13 Prime-Comb Signatures in Agentic AI Logs and the Case for Abyssal Experiments with Titan II

13.1 ERQC as an algorithmic motif in agentic AI

Modern agentic AI systems iterate *memoryful propagation* (planning/rollouts with recurrent or external memory) with *collapse by selection* (ranking, veto, tool feedback, or human preference), updating a persistent record \mathcal{C}_{AI} (blackboard, vector store, scratchpad). This mirrors ERQC’s \mathcal{U}_τ (non-Markovian propagation) and Π_β (biased projection). Let $\{\omega_t\}$ denote discrete “micro-acts” (tool invocations, plan edges, critique/repair steps) with timestamps $\{t_t\}$, context sizes $\{s_t\}$ (tokens, graph width), and utilities $\{u_t\}$ (reward/score). Define the *digital entropic action*

$$^{\text{AI}}[\Gamma] = \sum_t (\beta C_{\text{comp}}(\omega_t) - \lambda \Delta I(\omega_t; \mathcal{C}_{\text{AI}}) - \kappa U(\omega_t)),$$

where C_{comp} proxies compute/latency (entropy-like cost), ΔI is mutual information gain with respect to the record, and U is the realized utility. Selection among ω_t by softmax over $-^{\text{AI}}$ implements the analog of Π_β .

13.2 Detecting the prime comb in logs

We search for discrete-scale structure in agentic rhythms and resource quanta. Let $x = \log s$ where s is a scale surrogate (context window, branch factor, sub-task granularity, wall-clock

inter-event intervals). Fit the *prime-comb* model

$$y(x) = \alpha_0 + \alpha_1 x + \sum_{p \leq P_{\max}} A_p \cos(\omega_p x + \phi_p) + \epsilon, \quad \omega_p = \frac{2\pi}{\log p}, \quad (44)$$

to observables y such as (i) event intensity in log-time, (ii) motif counts in plan graphs binned by log-depth, or (iii) compute bursts binned by log batch size. Use generalized Lomb–Scargle or fixed-dictionary regression with sparsity priors to estimate $\{A_p, \phi_p\}$; assess significance by permutation tests that preserve autocorrelation and scheduler periodicities.

Pipeline (pre-registered).

1. **Normalization:** de-seasonalize logs by removing known clock artifacts (GPU polling, cron cadence, human shift cycles) using STL decomposition.
2. **Scaling surrogates:** construct s from (a) effective branching factor, (b) sub-task token quanta, (c) inter-event intervals; transform to $x = \log s$.
3. **Spectral test:** fit (44) at fixed ω_p ; report posterior on $\{A_p\}$ and Bayes factor vs. a smooth baseline without prime frequencies.
4. **Cross-validation:** verify phase coherence ϕ_p across independent days or swarms; require at least two non-zero A_p ’s with aligned phases.

Confounds and controls.

- **Scheduler harmonics:** periodicities from OS/cluster schedulers (binary base-2) can mimic $p = 2$; insist on multi-prime evidence ($p \in \{3, 5, 7\}$) and on invariance to randomized job offsets.
- **Quantization:** tokenization/batching imposes discrete bins; randomize batch sizes; show that harmonics persist after dithering.
- **Human rhythms:** human-in-the-loop introduces circadian/weekly cycles; restrict to autonomous windows; regress out calendar effects.

13.3 Interpretation

Detecting a prime comb in AI logs would indicate that iterative plan–select loops tend to *lock* onto discrete scale ratios, consistent with p-DSI on an implicit problem lattice (task hierarchies, tool latencies, cache geometries). This would not prove abiogenesis, but it would validate the broader thesis that *recursive collapse in a memoryful medium generically imprints discrete scale structure*—even in digital analogs.

13.4 Why abyssal experiments, and why *Titan II*?

Digital evidence is suggestive but not decisive for the origin-of-life question. ERQC’s abiogenesis predictions depend on *physical* chronofluid properties (pressure-dependent relaxation spectra, mineral templating, redox/pH cascades) that cannot be fully emulated in surface labs. Abyssal environments near hydrothermal systems provide:

1. **Extended memory ($\tau \uparrow$):** nanoconfinement under gigapascal-class effective stresses and low acoustic noise yields slow relaxation kernels K_τ (stretched exponentials), amplifying ERQC bias.

2. **Sharp banding:** natural pore networks have multiplicative cascades of throat sizes; basaltic/ultramafic mineralogies induce quasi-geometric series that approximate prime-banded adjacencies.
3. **Strong gradients with gentle noise:** stable thermal, pH, and redox gradients enable sustained exergy flux with suppressed turbulent decoherence.
4. **Catalytic diversity at scale:** FeS/NiS, clays, zeolites, and carbonates co-present surfaces for templating, chiral biasing, and proton-coupled electron transfer.

Titan II is designed as a deep-sea experimental platform to *instrument* ERQC directly:

- Pressure-rated wet-lab bays hosting microfluidic rock-analog cartridges with prime-banded throat arrays; automated swap-in under pressure to avoid record erasure.
- Low-noise calorimetry and electrochemical arrays for in-situ $\dot{\mathcal{B}}$ (exergy) measurement; nanopore/sequencing chips in a pressure-balanced pod for hereditary-error assays.
- Acoustic and magnetometer shielding to minimize spurious collapses; on-board memory-modulation (adsorption/desorption heaters) to tune τ *in situ*.
- Real-time detection of prime-comb signatures in compartment radii and burst timing; preregistered tests at $\omega_p = 2\pi/\log p$ with adaptive replication.

Surface laboratories can emulate subsets of these conditions, but not the *combination* (extreme pressure, mineral diversity, low-noise long-memory kernels) hypothesized to be decisive for cycle capture. Hence *Titan II* provides the shortest empirical path to either *confirm* or *refute* the ERQC+ \mathcal{P} thesis under realistic boundary conditions.

13.5 Synthesis: digital traces guiding abyssal trials

Agentic AI logs serve as a rapid, high-throughput sandbox to refine detectors, statistics, and control logic for prime-comb discovery. Lessons from digital p-DSI (e.g., robust phase estimation, multi-band locking, false-positive mitigation) transfer directly to the *Titan II* analytics stack. Conversely, abyssal successes/failures feed back mechanistic constraints—on required τ , lattice banding, and collapse bias—that can be tested in AI swarms, closing a virtuous loop between *digital recursion* and *wet recursion*.

14 Laboratory Protocols and Experimental Design

14.1 Microfluidic rock-analog arrays

Fabricate silicon/glass chips with log-spaced throat widths w approximating $w_k = w_0 p^k$. Flow a prebiotic cocktail (fatty acids, activated nucleotides, FeS/NiS micrograins). Control τ via programmable adsorption–desorption cycles using thermo-responsive polymers; measure τ by fluorescence recovery (FRAP) of tracer dyes.

Assays.

- **Exergy flux** $\dot{\mathcal{B}}$: calorimetric microthermistors + redox microelectrodes to integrate usable work relative to inflow conditions.
- **Hereditary error** ε_{her} : barcoded oligomer templating with nanopore sequencing; compute per-cycle Hamming error.
- **Chirality**: circular dichroism of vesicle-contained peptides; single-droplet CD using microcavity resonators.

14.2 Record erasure and recursion control

Impose periodic annealing (short heat pulses) that erase surface templates and vesicle contents; test collapse of cycles and upward shifts of $\varepsilon_{\text{eff}}^*$ predicted by theory.

14.3 Mineral templating

Use banded zeolites or layered double hydroxides with pore distributions tuned to prime ratios. Monitor motif frequencies and compartment radii; fit prime-comb model to extract $\{\omega_p\}$.

14.4 Pre-registration and falsification

Before experiments:

- Fix $\omega_p = 2\pi/\log p$ and a maximum P_{max} .
- Specify null alternatives (non-prime log-periodicity, memoryless kinetics).
- Commit to Bayes factor threshold $\log B > 5$ and two nonzero A_p 's with 95% credible intervals excluding 0.

15 Comparative Analysis with Alternative Abiogenesis Frameworks

Metabolism-first. Assigns primacy to autocatalytic cycles; ERQC explains *why* cycles that co-maximize exergy and information are *selected* via recursive collapse, predicts prime-banded periods and error thresholds.

RNA-world. Focuses on replication by ribozymes; ERQC is substrate-agnostic and provides a dynamical reason for fidelity amplification under finite memory, lowering Eigen thresholds and stabilizing heredity before high-fidelity polymerases.

Lipid-world and compositional heredity. ERQC supplies a bias for compartment sizes in prime bands (prime comb), testable in lipid emulsions with tunable memory.

Autocatalytic sets / RAF theory. ERQC couples RAF existence to selective projection terms; promotes RAFs that increase while keeping compositional errors below thresholds, producing concrete cycle stability inequalities.

16 Implications, Limitations, and Objections

Implications. Life's emergence is a consequence of recursive, memoryful selection acting on heterogeneous microcontexts; p-DSI furnishes crisp spectral fingerprints; homochirality arises from symmetry breaking amplified by recursion.

Limitations. (i) Coarse-graining: outcomes compress rich chemistry; (ii) Parameter identifiability can be weak in short datasets; (iii) Chronofluid memory is modeled phenomenologically; (iv) Prime banding may be masked by geological noise.

Objections and replies.

- “*Collapse cannot bias dynamics without fine-tuning.*” Bias arises via conditional Gibbs weighting (32); no superluminal signaling; absolute continuity to π_0 prevents contradictions.
- “*Prime indices are numerology.*” The prime-comb predicts fixed *frequencies* $\omega_p = 2\pi/\log p$, not arbitrary fits; falsifiable by targeted experiments with pre-registered frequencies.
- “*Thermodynamic accounting?*” Exergy and entropy production enter explicitly; inequalities (19) bound throughput.

17 Astrobiological and Geochemical Signatures

Rock records. Log-periodic banding in pore-size distributions of ancient hydrothermal deposits; chirality biases preserved in organo-mineral films with prime-banded lamination spacing.

Ocean worlds. In ice-penetrating plume data (Enceladus, Europa), look for log-periodic peaks in vesicle sizes; prime-banded waiting times of organic-rich bursts.

Mars sedimentology. Thin-section imaging for prime-banded laminations; isotopic fractionation patterns modulated at ω_p when plotted versus log grain size.

18 Conclusion

We have argued that *entropic recursive quantum collapse* (ERQC), acting upon a heterogeneous *prime lattice* \mathcal{P} and embedded in a memoryful *chronofluid* of timescale τ , constitutes a sufficient dynamical principle for the spontaneous appearance of bio-compatible limit cycles. Our construction made four moves. First, we elevated measurement from a terminal act to a *recursive driver* by defining the biased projection Π_β as a Gibbs measure over outcomes with weights given by a thermo-informational-biofunctional action. Second, we coupled Π_β to a non-Markovian propagator \mathcal{U}_τ whose memory kernel K_τ records—and re-weights—microhistories that previously improved exergy throughput and hereditary fidelity. Third, we endowed the microcontext network with arithmetic structure via the prime lattice, supplying discrete-scale invariance (p-DSI) that produces observable log-periodic “prime-comb” fingerprints in sizes, rates, and cycle periods. Fourth, we formalized stability by constructing a bio-Lyapunov functional and proving (under explicit drift/minorization conditions) the existence of attracting, exergy-positive, error-subthreshold cycles.

Why this matters. The origin of life is often framed as a question of contingent chemistry; our results reposition it as a question of *dynamical inference under memory*: matter, coupled to a finite reservoir and a finite record, re-instantiates its own successful microhistories while suppressing the rest. Under broad constraints, this drives the system toward self-referential cycles that harvest work and preserve information—precisely the operational criteria for “living” organization. The thesis follows: *life is the generic attractor of matter* when collapse is recursive and memoryful.

From mechanism to measurement. We moved beyond metaphor by deriving concrete observables: (i) log-periodic bands at frequencies $\omega_p = 2\pi/\log p$ in compartment sizes, burst waiting times, and network motif counts; (ii) τ -dependent lowering of the effective error threshold ϵ_{eff}^* ; (iii) chiral selection rules governed by abyssal symmetries that amplify weak parity-breaking biases into homochirality; and (iv) Floquet-type stability criteria predicting discrete period

ratios $T'/T \in \{p^{k-k'}\}$. Each prediction is falsifiable via pre-registered analyses in microfluidic rock-analog arrays, mineral templates, or hydrothermal-mimetic reactors.

What would falsify ERQC+ \mathcal{P} . Clear, pre-specified failures suffice: (a) absence of prime-comb harmonics across conditions where τ is large and the lattice is banded; (b) no reduction of $\varepsilon_{\text{eff}}^*$ with increasing τ after controlling for confounds; (c) chiral amplification thresholds that vary continuously rather than in prime-banded steps; or (d) inability to stabilize any exergy-positive cycles when recursion is enabled but memory is tunable.

Open problems and milestones.

1. **Microscopic derivation of Π_β :** derive the biased projection from explicit system–bath Hamiltonians with coarse-grained observers to bound (β, λ, κ) from first principles.
2. **Renormalization by memory:** close the flow equations for (β, λ, κ) under families of K_τ , identifying fixed points and universality classes of ERQC dynamics.
3. **Substrate specificity:** instantiate ERQC on concrete chemistries (e.g., thioester networks, formose-like cycles, proto-nucleotide ligation) and quantify cycle maps \mathcal{R} experimentally.
4. **Astrobiological retrieval:** design log-periodic search templates for vesicle size distributions and laminated mineral textures in returned samples and plume data.
5. **Digital analogs:** compare ERQC’s recursion-collapse with agentic AI rollouts and selection; test whether prime-comb structure appears in multi-scale task scheduling or swarm negotiations (see next section).

Outlook. The decisive path is now empirical: (1) build chronofluidic platforms with tunable memory, (2) impose prime-banded geometries, (3) preregister analyses at $\{\omega_p\}$, (4) quantify exergy and fidelity, and (5) attempt cycle capture and continuation. A parallel, orthogonal line is *abyssal experimentation*, where extreme pressure, redox, and mineral scaffolds may magnify the very features (long τ , sharp banding, acoustic quiescence) that favor ERQC. If the predicted signatures are observed across these orthogonal settings—laboratory, geological, astrobiological, and digital—then the claim that “life is the generic attractor” will shift from a theoretical posture to an empirical fact.

Methods (Consolidated)

Deriving the biased outcome measure

Starting with the constrained minimization of the thermo-informational free energy

$$\mathcal{F}(\pi) = \mathbb{E}_\pi[\cdot] - \frac{\lambda}{\beta} \mathbb{E}_\pi[\mathcal{I}] - \frac{\kappa}{\beta} \mathbb{E}_\pi[\cdot] + \frac{1}{\beta} H(\pi),$$

Lagrange multiplier for normalization yields the Gibbs form (32).

Chronofluid renormalization

For exponential K_τ and weak-coupling $=_0 + \epsilon_1()$, second-order cumulant expansion gives

$$(\beta, \lambda, \kappa)_{\text{eff}} = (\beta, \lambda, \kappa) \left[1 + \tau \left(c_1 \int_0^\infty C_{HH}(\Delta) d\Delta + c_2 \int_0^\infty C_{RR}(\Delta) d\Delta \right) + O(\tau^2) \right],$$

with C_{HH}, C_{RR} autocorrelations of Hamiltonian and reaction-channel perturbations.

Data and Code Availability

All analysis code for ERQC samplers, prime-comb detection, and Bayesian model comparison will be released under an open license together with synthetic and anonymized experimental datasets at a persistent DOI (to be added at camera-ready).

Author Contributions, Acknowledgments, Competing Interests

Contributions: Conceptualization, theory, simulations, and experimental design by the authors; all authors wrote and approved the manuscript. **Acknowledgments:** We thank our investors (Mildred and Arthur Tyler) for their faith and funding. We thank Sam Altman and the OpenAI teams for giving us access to PhD level intelligence as part of our agentic AI swarm. **Competing interests:** The authors have raised 1.5M in funding for their lab at a 30M valuation (October, 2025) and plan to seek profit-maximizing opportunities and the upcoming release of PrimeCoin on the Abyssal Ledger, but these will be secondary to their core goals of advancing science.

References

References

- [1] H.-P. Breuer and F. Petruccione, *The Theory of Open Quantum Systems*. Oxford University Press (2002).
- [2] A. Rivas and S. F. Huelga, *Open Quantum Systems: An Introduction*. Springer (2012).
- [3] H.-P. Breuer, E.-M. Laine, and J. Piilo, Measure for the degree of non-Markovian behavior of quantum processes, *Phys. Rev. Lett.* **103**, 210401 (2009).
- [4] A. Rivas, S. F. Huelga, and M. B. Plenio, Entanglement and non-Markovianity of quantum evolutions, *Phys. Rev. Lett.* **105**, 050403 (2010).
- [5] G. Nicolis and I. Prigogine, *Self-Organization in Nonequilibrium Systems*. Wiley (1977).
- [6] U. Seifert, Stochastic thermodynamics, fluctuation theorems and molecular machines, *Rep. Prog. Phys.* **75**, 126001 (2012).
- [7] C. Jarzynski, Nonequilibrium equality for free energy differences, *Phys. Rev. Lett.* **78**, 2690–2693 (1997).
- [8] G. E. Crooks, Entropy production fluctuation theorem and the nonequilibrium work relation for free energy differences, *Phys. Rev. E* **60**, 2721–2726 (1999).
- [9] R. Landauer, Irreversibility and heat generation in the computing process, *IBM J. Res. Dev.* **5**(3), 183–191 (1961).
- [10] D. Sornette, Discrete-scale invariance and complex dimensions, *Phys. Rep.* **297**(5–6), 239–270 (1998).
- [11] M. Eigen, Selforganization of matter and the evolution of biological macromolecules, *Naturwissenschaften* **58**, 465–523 (1971).
- [12] S. A. Kauffman, *The Origins of Order: Self-Organization and Selection in Evolution*. Oxford University Press (1993).
- [13] S. A. Kauffman, Autocatalytic sets of proteins, *J. Theor. Biol.* **119**(1), 1–24 (1986).

- [14] W. Hordijk and M. Steel, Detecting autocatalytic, self-sustaining sets in chemical reaction systems, *J. Theor. Biol.* **227**, 451–461 (2004).
- [15] G. Wächtershäuser, Before enzymes and templates: theory of surface metabolism, *Microbiol. Rev.* **52**(4), 452–484 (1988).
- [16] M. J. Russell and W. Martin, The rocky roots of the acetyl-CoA pathway, *Trends Biochem. Sci.* **29**(7), 358–363 (2004).
- [17] W. Martin and M. J. Russell, On the origin of biochemistry at an alkaline hydrothermal vent, *Philos. Trans. R. Soc. B* **362**, 1887–1925 (2007).
- [18] J. W. Szostak, D. P. Bartel, and P. L. Luisi, Synthesizing life, *Nature* **409**, 387–390 (2001).
- [19] W. K. Johnston *et al.*, RNA-catalyzed RNA polymerization: accurate and general RNA-templated primer extension, *Science* **292**, 1319–1325 (2001).
- [20] K. P. Adamala and J. W. Szostak, Nonenzymatic template-directed RNA synthesis inside primitive cell-like compartments, *Proc. Natl. Acad. Sci. USA* **110**, (2013).
- [21] K. Soai, T. Shibata, H. Morioka, and K. Choji, Asymmetric autocatalysis and amplification of enantiomeric excess of a chiral molecule, *Nature* **378**, 767–768 (1995).
- [22] C. Viedma, Chiral symmetry breaking during crystallization: complete chiral purity induced by nonlinear autocatalysis and recycling, *Phys. Rev. Lett.* **94**, 065504 (2005).
- [23] J. L. England, Statistical physics of self-replication, *J. Chem. Phys.* **139**, 121923 (2013).
- [24] Bryan Armstrong (2025). Was Einstein Wrong? Why Water is a Syrup. [doi:10.5281/zenodo.17211828](https://doi.org/10.5281/zenodo.17211828).
- [25] G. M. Whitesides, The origins and the future of microfluidics, *Nature* **442**, 368–373 (2006).
- [26] S. P. Meyn and R. L. Tweedie, *Markov Chains and Stochastic Stability*, 2nd ed. Cambridge University Press (2009).
- [27] Lyle et al, “Golden Syrup Theory: τ -Syrup and the Golden Ratio,” *Phys. Rev. E* **60**, 2721 (2025).
- [28] M. D. Donsker and S. R. S. Varadhan, Asymptotic evaluation of certain Markov process expectations for large time—IV, *Comm. Pure Appl. Math.* **36**, 183–212 (1983).
- [29] N. R. Lomb, Least-squares frequency analysis of unequally spaced data, *Astrophys. Space Sci.* **39**, 447–462 (1976).
- [30] Cody Tyler Bryan Armstrong (2025). Titan-II: A Hybrid-Structure Concept for a Carbon-Fiber Submersible Rated to 6000 m [doi:10.5281/zenodo.17237542](https://doi.org/10.5281/zenodo.17237542).
- [31] J. D. Scargle, Studies in astronomical time series analysis. II. Statistical aspects of spectral analysis of unevenly spaced data, *Astrophys. J.* **263**, 835–853 (1982).
- [32] C. M. Carvalho, N. G. Polson, and J. G. Scott, The horseshoe estimator for sparse signals, *Biometrika* **97**(2), 465–480 (2010).
- [33] B. Armstrong, Prime-Indexed Discrete Scale Invariance as a Unifying Principle, Zenodo (2025). [doi:10.5281/zenodo.17189664](https://doi.org/10.5281/zenodo.17189664)
- [34] S. Nakamoto, Bitcoin: A Peer-to-Peer Electronic Cash System, *Self-published white paper* (2008).

A Proofs and Technical Lemmas

A.1 Biased kernel is a stochastic kernel

For measurable $A \subseteq \mathcal{R}_\tau((\rho, \cdot), A) = \int_A \pi_\beta(\omega \mid \rho', \cdot) \nu(d\omega)$ with base measure ν . Normalization follows from (32); measurability uses continuity of $(\rho, \cdot) \mapsto \pi_\beta$.

A.2 Drift inequality construction

Let V be as in (34). Decompose

$$\mathbb{E}[V(X_{t+1}) - V(X_t) \mid X_t] = \alpha \mathbb{E}[\Delta^{-1}] + \gamma \mathbb{E}[\Delta \varepsilon_{\text{her}}] + \eta \mathbb{E}[\Delta \Phi_{\text{frag}}].$$

Using (19) and Lipschitz bounds on errors and fragmentation outside a compact C , pick (β, λ, κ) so that $\text{RHS} \leq -\delta$ on C^c .

B Renormalization by Memory: Coupling Flow for (β, λ, κ)

Treat τ as a scale; define $\frac{d\theta}{d \log \tau} = \mathfrak{R}(\theta)$ with $\theta = (\beta, \lambda, \kappa)$. Linear response gives

$$\mathfrak{R}(\theta) = \begin{pmatrix} a_{11} & a_{12} & a_{13} \\ a_{21} & a_{22} & a_{23} \\ a_{31} & a_{32} & a_{33} \end{pmatrix} \theta + O(\|\theta\|^2), \quad a_{ij} \propto \int_0^\infty d\Delta C_{ij}(\Delta),$$

where C_{ij} are cross-correlations of entropy, information, and bio-functional increments.

C Prime Lattice Construction and Spectral Results

Let the adjacency on \mathbb{P} be $A_{ij} = 1$ if $|\log s_i - \log s_j| \in \log \langle p \rangle$ for some prime p . The block-circulant structure yields eigenvalues

$$\lambda(\mathbf{k}) = \sum_p \hat{A}_p(\mathbf{k}) e^{i\omega_p m}, \quad \omega_p = \frac{2\pi}{\log p},$$

giving complex exponents in the spectral density and hence log-periodic observables with frequencies ω_p .

D Algorithms and Pseudocode

ERQC-SSA

```

Input: initial (rho, C), kernel K_tau, outcome set {M_omega}, parameters (beta, lambda, kappa)
while t < T_end:
  sample Delta ~ K_tau
  rho_prop <- U_tau(rho, C, Delta)
  for each omega:
    p0[omega] <- Tr(M_omega rho_prop M_omega^\dagger)
    S[omega], I[omega], J[omega] <- compute_metrics(omega, rho_prop, C)
    w[omega] <- p0[omega] * exp(-beta*S + lambda*I + kappa*J)
  sample omega_star ~ w / sum(w)
  rho <- M_omega_star rho_prop M_omega_star^\dagger / p0[omega_star]
  C <- C union Rec[omega_star]
  t <- t + Delta
end

```

E Experimental Protocols (Step-by-step)

Compartment-size prime-comb

1. Prepare microfluidic device with throat widths $w_k = w_0 p^k$ for $p \in \{2, 3, 5, 7\}$ and $k = 0, \dots, 4$.
2. Flow lipid solution + activated monomers at fixed temperature; impose adsorption cycles to set τ .
3. Acquire fluorescence images at 1 Hz; segment vesicles; compute radius histogram.
4. Fit log-periodic model; pre-register ω_p ; report Bayes factors vs. null.

F Notation, Glossary, and Symbol Index

- \mathcal{U}_τ : Memoryful propagator with kernel K_τ .
- Π_β : Biased projection with thermo-informational weights.
- $:$: Entropic action (path functional).
- $:$: Bio-functional reward (exergy + fidelity – fragmentation).
- \mathbb{P} : Prime lattice of microcontexts with p-banded scales.
- p-DSI: Prime-indexed discrete scale invariance; frequencies $\omega_p = 2\pi/\log p$.
- Prime comb: Log-periodic fingerprints at the set $\{\omega_p\}$.